

Design and Chromatic Aberration Analysis of Plasmonic Lenses Using the Finite Element Method

Cosme E. Rubio-Mercedes, Vitaly F. Rodríguez-Esquerre, *Member, IEEE*, Ivan T. Lima, Jr., *Senior Member, IEEE*, and Hugo E. Hernández-Figueroa, *Senior Member, IEEE*

Abstract—We designed plasmonic lenses and analyzed their chromatic aberration using the finite element method (FEM) in frequency domain with perfectly matched layers (PML). Plasmonic lenses permit subwavelength focusing of light in the visible and in the near infrared. The focal distance of these devices depends on the wavelength operation due to the dispersive characteristics of the lens structures and the refractive index of their constituent materials. With a uniform incident wave normal to the lens surface, focusing of light by surface plasmon polariton (SPPs) through a plasmonic lens is obtained in the axial direction. The design of three plasmonic lenses in Silver (Ag), Gold (Au) and Copper (Cu) films at two central operation wavelengths of 650 nm and 810 nm, in both, cylindrical and rectangular geometries were considered and the chromatic aberration of the lenses were analyzed by monitoring the peak position of the electromagnetic (EM) field when the wavelength changes from 625 nm to 675 nm and from 785 nm to 835 nm..

Index Terms—Chromatic aberration, finite element method, numerical analysis, plasmonic lenses, surface plasmon polaritons.

I. INTRODUCTION

PLASMONIC lenses are devices that permit the focusing of light in the visible and near infrared in sub wavelength regions [1]–[3]. At optical frequencies, these structures can be implemented by alternating nanocapacitors and nanoinductors that can be built using dielectric and plasmonic nanostructures, respectively [5]–[7]. Optical lenses are excellent candidates for coupling light between two optical devices such as sources and waveguides or fiber and nanowaveguides. Silver (Ag), Gold (Au) and Copper (Cu) are the most prominent materials that can be used for lenses fabrication. Since metals are very dispersive

Manuscript received June 26, 2012; revised December 02, 2012; accepted January 06, 2013. This work was supported in part by CAPES (Process number 3724/10-7), in part by CNPq (INCT Fotonicom Process number 305992/2005-8, 471658/2007-3, and 302390/2009-0), and in part Optics and Photonics Research Center (CEPOF) under Grant 05/51689-2, Fapesb and UFBA. Date of publication January 22, 2013; date of current version February 13, 2013.

C. E. Rubio-Mercedes is with the Mathematics and Engineering Physics Programs, State University of Mato Grosso do Sul-UEMS, Dourados-MS 79804-970, Brazil (e-mail: cosme@uems.br).

V. F. Rodríguez-Esquerre, is with the Department of Electrical Engineering at the Federal University of Bahia, Salvador, Brazil (e-mail: vitaly.esquerre@ufba.br).

I. T. Lima Jr. is with the Department of Electrical and Computer Engineering, North Dakota State University, Fargo, ND 58108 USA (e-mail: Ivan.Lima@ndsu.edu).

H. E. Hernández-Figueroa is with the Department of Microwaves and Optics, School of Electrical and Computer Engineering, University of Campinas, Unicamp, Campinas-SP 13083-970, Brazil (e-mail: hugo@dmo.fee.unicamp.br).

Color versions of one or more of the figures in this paper are available online at <http://ieeexplore.ieee.org>.

Digital Object Identifier 10.1109/JLT.2013.2241732

materials which exhibit very different values of complex refractive index depending on the operating wavelength, the lens characteristics, such its chromatic aberration and full-width at half maximum (FWHM), should be analyzed for polychromatic illumination operation.

In this article, we designed plasmonic lenses and numerically analyzed the chromatic aberration of these structures made of three different materials: Ag, Au, and Cu. The chromatic aberration of plasmonic lenses is the result of the combination of the lens structure dispersion and the material dispersion due to the wavelength dependence of the refractive index of the constituent material. In subwavelength imaging, chromatic aberration can be seen as fringes of color around the image. We consider the design principle on plasmonic lenses for rectangular coordinates introduced in [1], [2] and adapted to cylindrical coordinates [11], [12]. Light focusing is achieved by constructing a carefully designed phase front retardation for the plasmonic lenses. The control of the phase front profile is achieved through phase retardation caused by the width and position of individual cylindrical apertures in the lens. The simulations were carried out using an efficient two dimensional finite element method (2D-FEM) in frequency domain in rectangular [9], [10] and in cylindrical [11], [12] coordinates. After we calculated the field distribution in these structures we obtained the maximum field position (z_{\max}) of the focused light which depends on the operating wavelength due the chromatic aberration. In the simulation, to analyze the chromatic aberration we are taking into account both, the lens structure dispersion and the material dispersion.

The lenses analyzed consist of several concentric cylindrical nano-apertures in metallic films as shown in Fig. 1. The normal incident light propagates along the cylindrical nano-plasmonic lenses and by a judicious choice of the nanoslit widths the phase shift can be controlled to produce a constructive interference of light at a focal distance f [1], [2]. We also analyzed rectangular lenses that consist of parallel slits, which produce a focused line at the focal distance, using the 2D-FEM in rectangular coordinates.

II. DESIGN OF PLASMONIC LENSES

To numerically simulate the electromagnetic (EM) field in plasmonic lenses, we considered a general three dimensional structure with cylindrical symmetry as shown in Fig. 1. This design consists of several concentric cylindrical nano-apertures with different widths and radial positions in a metallic film. Due to the cylindrical symmetry of the structures with respect to the axial direction, we reduced the computational domain to the r - z plane, from $r = 0$ to the radius of the lens, as shown in Fig. 2.

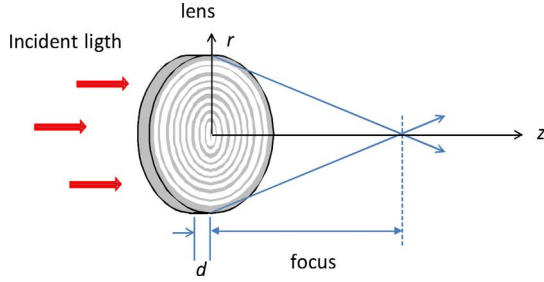


Fig. 1. Schematics of a plasmonic lens that consists of concentric cylindrical nano-apertures in a metallic film.

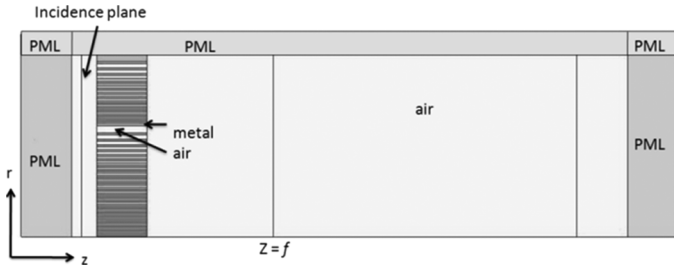


Fig. 2. Two dimensional computational scheme for cylindrical and rectangular simulation of EM waves in plasmonic lenses.

As a result of the geometry of the lens and the incident EM field, we assume that there is no variation of the field along the other transversal coordinate for both the cylindrical formulation, applied to the cylindrical lens, and the rectangular formulations, applied to the rectangular lens. The two dimensional (2D) computational scheme of Fig. 2 can be used to simulate plasmonic lenses in cylindrical and rectangular coordinates [8]–[12]. The Perfectly Matched Layers (PMLs) are used to simulate open boundaries and to avoid reflections that are not desirable in the computational domain.

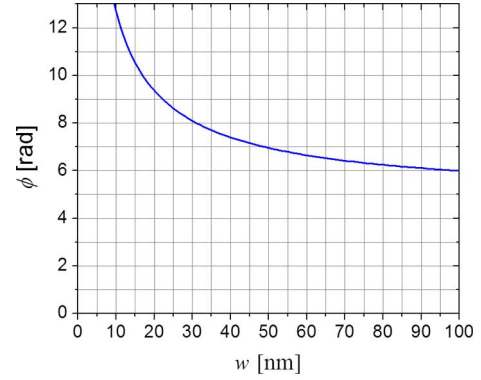
The propagation constants, β , which is related to the phase retardation of PPS propagated in a metal-dielectric-metal waveguides, can be expressed by the transcendental equation [1]–[3]:

$$\tanh\left(\sqrt{\beta^2 - k_0^2 \varepsilon_d} \frac{w}{2}\right) = -\frac{\varepsilon_d \sqrt{\beta^2 - k_0^2 \varepsilon_m}}{\varepsilon_m \sqrt{\beta^2 - k_0^2 \varepsilon_d}} \quad (1)$$

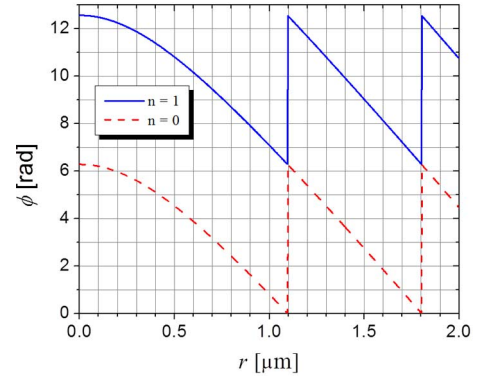
where k_0 is the wave vector of the light in free space, w is the waveguide width, and ε_d and ε_m are the relative permittivity of dielectric and the metal, respectively. The complex nature of the propagation constant due to the metals operating at optical frequencies has been considered. The values of β were obtained by using an iterative process for surface plasmon polariton (SPP) propagation in waveguides with variant slit width. The real and imaginary parts of β determine the phase velocity and the propagation loss of SPPs inside the metallic aperture, respectively.

The phase change of the light transmitted through the aperture is expressed as

$$\phi = \text{Re}[\beta d] + \theta \quad (2)$$



(a)



(b)

Fig. 3. (a) Phase shift as a function of the width for a metallic waveguide of Ag with $d = 500$ nm calculated using (2). (b) Phase shift necessary at the output wave as a function of the radial position calculated using (4).

where θ represents the multiple light reflection between the entrance and exit interfaces and it can be calculated from the following equation:

$$\theta = \arg\left[1 - \left(\frac{k_0 - \beta}{k_0 + \beta}\right)^2 e^{2j\beta d}\right] \quad (3)$$

Equations (1) and (2) indicate that the phase change depends on the lens depth, the width of the apertures, the wavelength and the complex permittivity of the metal. Previous numerical results [1]–[3] showed that only the real part of βd represents a dominating contribution for the phase change. Therefore, ϕ can be approximated by $\text{Re}(\beta d)$, and its value can be controlled by varying β and d independently, which correspond to different lengths and widths respectively. The propagation constant was computed using (1), with $d = 500$ nm, and the metal Ag was used with a relative permittivity $\varepsilon_m = -17.0234 + j1.1518$ at the wavelength 650 nm [12] and $\varepsilon_d = 1$ for air. Fig. 3(a) shows the geometric dependence of the phase change as a function of the slits width w , between 10 nm and 100 nm, calculated using (2).

The principle of operation of the lens consist in introducing a phase shift on the incident wave at the output of the cylindrical array of rings by a proper choice of the parameters of the following equation,

$$\phi(r) = 2n\pi + \frac{2\pi f}{\lambda} - \frac{2\pi\sqrt{f^2 + r^2}}{\lambda} \quad (4)$$

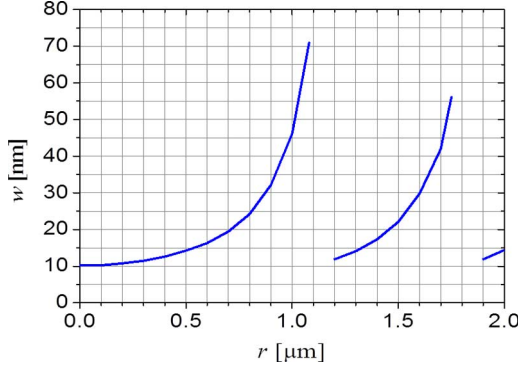


Fig. 4. Distribution of cylindrical slit width of air as a function of the radial position on the designed plasmonic lens calculated using (2) and (4). The metallic film used was Ag at the wavelength 650 nm and the film thickness was $d = 500$ nm.

TABLE I
RELATIVE PERMITTIVITY VALUES OF SILVER, COPPER AND GOLD AT 650 NM AND 810 NM.

Material	650 nm	810 nm
Silver	-17.0234 + 1.1518i	-28.7992 + 1.5375i
Gold	-9.7814 + 1.0492i	-27.2964 + 1.9144i
Copper	-13.2049 + 1.5646i	-26.1920 + 2.7027i

where n is an integer number, f is the focal distance measured from the output of the lens, r is the radial distance, and λ is the incident wavelength. The phase change necessary at the output of the lens as a function of the radial position r to focus the light at $f = 600$ nm is calculated using (4) and shown in Fig. 3(b).

Using (2) and (4), we calculate the slit width as a function of the radial position r between $0 \mu\text{m}$ and $2 \mu\text{m}$ for Ag at the wavelength of 650 nm and it is shown in Fig. 4. The freedom to determine the position and width of the slits were the design parameters. Metallic regions with width smaller than 24 nm should be avoided to prevent the occurrence of SPP crosstalk between adjacent apertures.

The relative permittivity values at the wavelengths 650 nm and 810 nm used in the plasmonic lens design for the materials that we considered are shown in Table I. The relative permittivity values for these materials at the other wavelength that we investigated are obtained using equations given in [8].

III. METHOD OF ANALYSIS

In order to calculate the field distribution of plasmonic lenses, we use the frequency domain 2D-FEM in both rectangular [9], [10] and cylindrical [11], [12] formulations for the lens that consists of rectangular slits and cylindrical slits, respectively. This numerical technique is, within certain limits of applicability, reliable and accurate, particularly for non continuous structures. To reduce the computational domain we used the Perfectly Matched Layers (PML) in the simulations. In this section we briefly outline the method for cylindrical coordinates to model cylindrical slits [11], [12]. The method used for rectangular coordinates to model rectangular slits is analogous and can be found in [9], [10].

Wave propagation in plasmonic lenses, such as in Fig. 1, is described by the Helmholtz type equation in cylindrical coordinates

$$\frac{s_r}{r} \frac{\partial}{\partial r} \left(p r \frac{s_r}{s} \frac{\partial \phi}{\partial r} \right) + s_z \frac{\partial}{\partial z} \left(p \frac{s_z}{s} \frac{\partial \phi}{\partial z} \right) + k_0^2 q s \phi = 0 \quad (5)$$

where $p = 1$, $q = \varepsilon(y, z)$, $\phi = \phi_r$ is the scalar field, and $\varepsilon(y, z)$ is the relative permittivity. The parameter s_r , s , and s_z are related to PMLs adapted for cylindrical coordinates [11], [12].

Applying the Galerkin procedure to (1), the following matrix equation is obtained

$$[A] \{\varphi\} = -2\beta [B] \{\varphi_{\text{inc}}\} \quad (6)$$

where $[A]$ is the resulting assembled global matrix given by

$$[A] = \sum_e \int_{\Omega_e} \left[p \frac{s_r^2}{s} r \frac{\partial \{N\}}{\partial r} \frac{\partial \{N\}^T}{\partial r} + p \frac{s_z^2}{s} r \frac{\partial \{N\}}{\partial z} \frac{\partial \{N\}^T}{\partial z} - k_0^2 q s r \{N\} \{N\}^T \right] dr dz \quad (7)$$

where β is the effective propagation constant of the waveguide, $\{\varphi_{\text{inc}}\}$ is the incident field and $[B]$ is the resulting matrix of the one dimensional (1D) FEM applied in the incidence plane, which is given by

$$[B] = \sum_e \int_{\Omega_e} p r \frac{s_z^2}{s} \{N\} \{N\} dr \quad (8)$$

2D numerical integrations have been used to calculate the fundamental matrixes in order to model complex problems with curved shaped geometries.

IV. CHROMATIC ABERRATION ANALYSIS

To analyze the chromatic aberration, the plasmonic lenses have been designed at the operation wavelengths of 650 nm and 810 nm, and made of the following materials: Ag, Au, and Cu. The incident light is a uniform plane wave normal to the lens surface. The structures analyzed consist of plasmonic lenses with cylindrical slits and plasmonic lenses with rectangular slits, for which we used the same computational mesh of the geometry given in Fig. 2 with the cylindrical and the rectangular coordinates, respectively. Transverse magnetic (TM) mode waves were used in the rectangular formulation because the excitation requirements of the SPPs.

First, we considered three lenses designed to operate at the incident wavelength 650 nm for metallic materials of Ag, Au, and Cu. The computational domain was $0 \mu\text{m} \leq z \leq 4.5 \mu\text{m}$ and $0 \mu\text{m} \leq r \leq 2.5 \mu\text{m}$ divided in 37240 elements (74761 points), where the PMLs are the outer $0.5 \mu\text{m}$ regions. The depth d was equal to 500 nm for all lenses, they were located from $z = 0.7 \mu\text{m}$ to $z = 1.2 \mu\text{m}$, and their focal distances were designed to be $f = 0.6 \mu\text{m}$. At this wavelength the relative permittivities ε_m were $-17.0234 + 1.1518i$, $-9.7814 + 1.0492i$, and $-13.2049 + 1.5646i$ for Ag, Au, and Cu, respectively, based on [8]. The incidence plane is placed at $z = 0.6 \mu\text{m}$ and the EM field intensities distribution of the simulation results using the FEM for these simulations are shown in Fig. 5: (a) Ag, (b) Au, and (c) Cu. The peak position (z_{max}) at the focus spot were

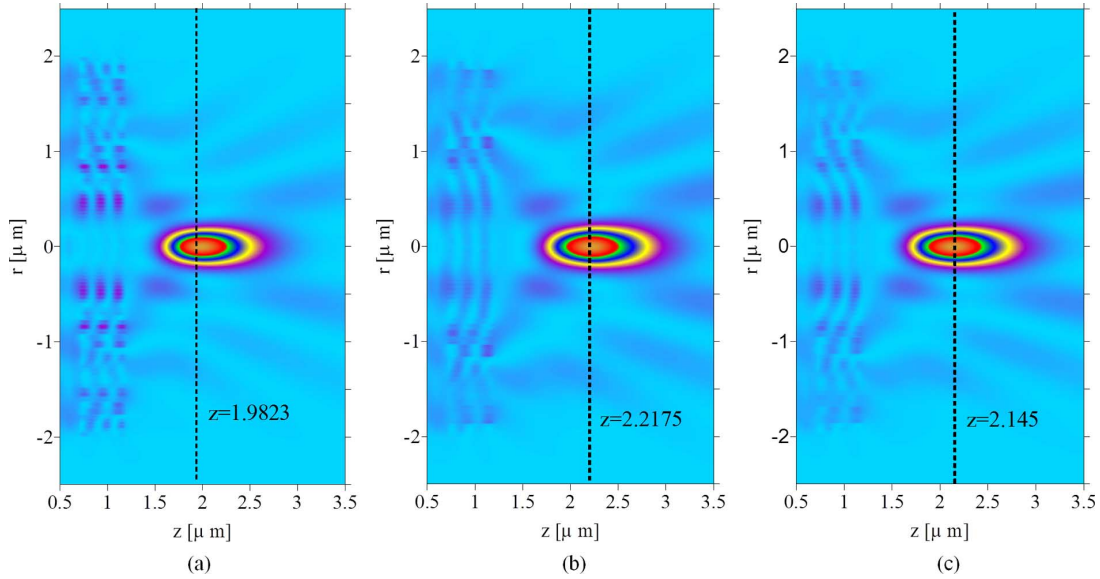


Fig. 5. EM field intensities of the simulation results using FEM for cylindrical plasmonic lenses at the wavelength 650 nm comprised of (a) Ag, (b) Au, and (c) Cu. The plane wave source was located at $z = 0.6 \mu\text{m}$ and the plasmonic lenses are located from $z = 0.7 \mu\text{m}$ to $z = 1.2 \mu\text{m}$.

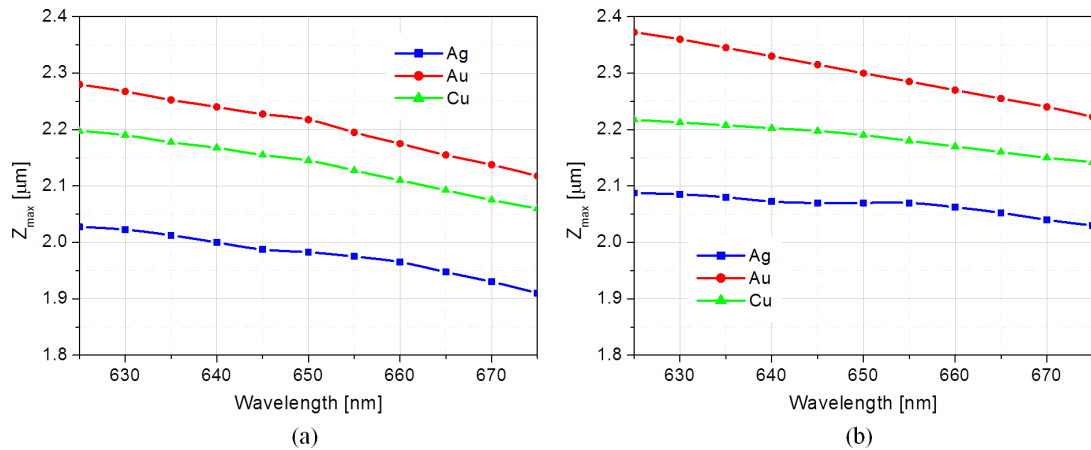


Fig. 6. Position (z_{max}) at the location with the highest EM field intensity produced by the plasmonic lenses comprised of Ag, Au, and Cu as a function of the wavelength from 625 nm to 675 nm for (a) cylindrical lens and (b) rectangular lens.

calculated and their values are $z = 1.9823 \mu\text{m}$, $z = 2.2175 \mu\text{m}$, and $z = 2.145 \mu\text{m}$ for Ag, Au, and Cu, respectively. These values are consistent with the focal distance designed. Since the lenses end is at $z = 1.2 \mu\text{m}$ and the focal distance was chosen as being $f = 0.6 \mu\text{m}$, the focal distances should start at $z = 1.8 \mu\text{m}$. The results are in agreement with the literature [12], in which a lens made of Ag was considered.

The peak positions of the EM focus spot, or focus line for the rectangular lens, for incident wavelengths varying from 625 nm to 635 nm were calculated and shown in Fig. 6(a-b). We updated the value of the permittivity values of the metallic materials at each wavelength [8]. In Fig. 6(a) and (b) we observed that the focal position (z_{max}) decreases by 200 nm when the wavelength increases from 625 nm to 675 nm. It is worth noting that, for this wavelength range, z_{max} decreases monotonically with the wavelength, and that Ag has the smallest focal distance z_{max} case in both cylindrical and rectangular lenses. We also observed that the rectangular lenses have the focal distance z_{max} significantly large when compared to the cylindrical lenses for the three metallic materials that we investigated.

We also designed nanoslit lenses to operate near the wavelength of 810 nm for Ag, Au, and Cu. At this wavelength the relative permittivities ϵ_m used were of $-28.7992 + 1.5375i$, $-27.2964 + 1.9144i$, and, $-26.1920 + 2.7027i$ for Ag, Au, and Cu, respectively [8]. All the other computational parameters are the same of the previous simulation example. The field intensities of the simulation results using the FEM for these simulations are shown in the Fig. 7: (a) Ag, (b) Au, and (c) Cu. The position (z_{max}) of highest EM field intensity were $z = 1.9525 \mu\text{m}$, $z = 1.9375 \mu\text{m}$, and $z = 1.96 \mu\text{m}$ for Ag, Au, and Cu, respectively.

The positions with the highest EM field intensity as a function of the incident wavelength from 785 nm to 835 nm were calculated and the results are shown in Fig. 8(a-b) for cylindrical and rectangular lenses, respectively. We observe that, when the operation wavelength values increase from 785 nm to 835 nm, the z_{max} values oscillate around the mean value for cylindrical formulation and monotonically decrease in the range of 60 nm in the rectangular counterpart. For the cylindrical lenses, the z_{max} values of the Cu lens is larger than the Ag lens and the z_{max}

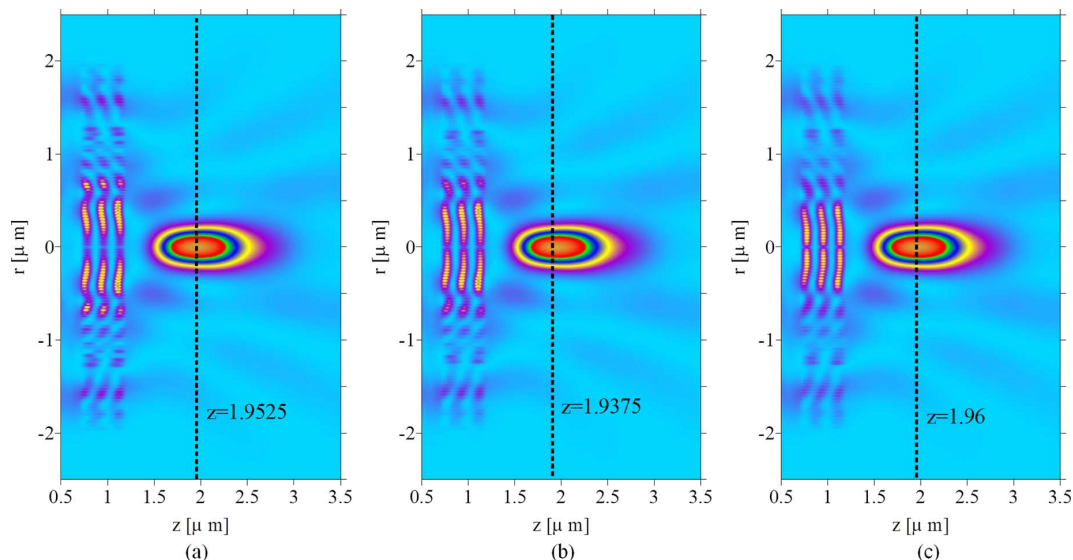


Fig. 7. EM field intensities of the simulation results using FEM for cylindrical plasmonic lenses at the wavelength 810 nm comprised of (a) Ag, (b) Au, and (c) Cu. The plane wave source was located at $z = 0.6 \mu\text{m}$ and the plasmonic lenses are located from $z = 0.7 \mu\text{m}$ to $z = 1.2 \mu\text{m}$.

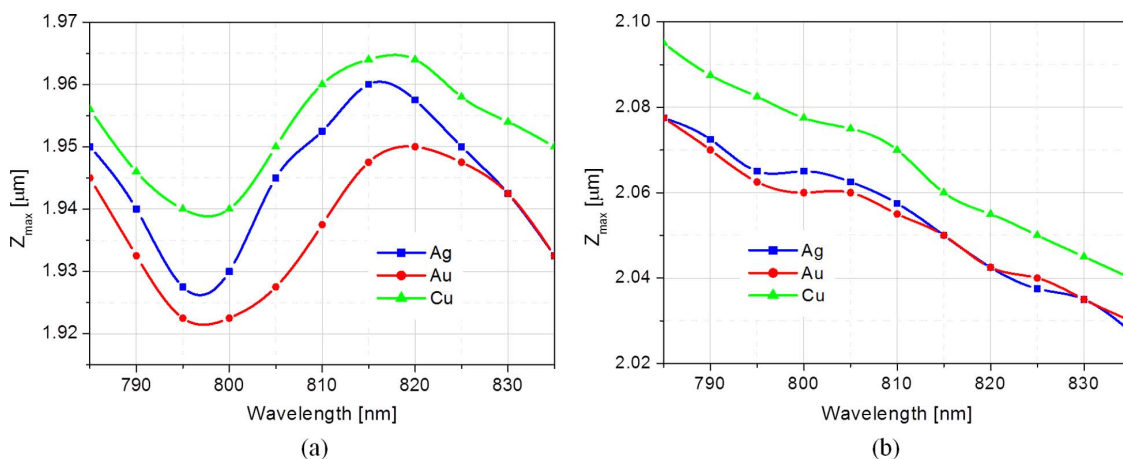


Fig. 8. Position (z_{max}) with the highest EM field intensity produced by the plasmonic lenses comprised of Ag, Au, and Cu as a function of the wavelength from 785 nm to 835 nm for (a) cylindrical lens and (b) rectangular lens.

values of the Au are shorter than the Ag lens in all spectral domain. For the rectangular lenses, the z_{max} values of the Cu lens are the largest, and Au and Cu lenses present near the same wavelength dependence of the focal distance.

In all the simulation, the full-width at half maximum (FWHM) at z_{max} exhibits a constant value of about 0.47λ for the cylindrical lenses.

We designed cylindrical and rectangular nanoslit plasmonic lenses and analyzed the chromatic aberration of these lenses operating in the visible and infrared using the 2D-FEM in the frequency domain using cylindrical and rectangular coordinates. The plasmonic lenses were made of Ag, Au, and Cu at the central operation wavelength of 650 nm and 810 nm.

V. CONCLUSIONS

We showed the wavelength dependence of the position (z_{max}) with the highest EM field intensity taking into consideration the

lens geometry and the optical characteristics of the metallic materials considered. We observed a significant variation of the wavelength dependence of the position (z_{max}) with the highest field intensity in the nanoslit lenses that we analyzed along the propagation direction when the incident light wavelength changes from 625 nm to 675 nm and from 785 nm to 835 nm. Therefore, different nanoslit lens designs that minimize this chromatic aberration have to be investigated if plasmonic lenses are being considered for coupling between optical devices or subwavelength imaging. A general procedure for designing a near-field plate given a desired image is discussed in [5]–[7], its implementation at optical frequencies can be obtained with ingenious configuration of nanoinductors, nanocapacitors in the transverse direction of the plasmonic lens. Several other plasmonic lens configurations, including metallic photonic crystals [4], are under analysis and results will be reported in the future.

REFERENCES

- [1] H. Shi, C. Wang, C. Du, X. Luo, X. Dong, and H. Gao, "Beam manipulating by metallic nano-slits with variant widths," *Opt. Exp.*, vol. 13, pp. 6815–6820, 2005.
- [2] T. Xu, C. Du, C. Wang, and X. Luo, "Subwavelength imaging by metallic slab lens with nanoslits," *Appl. Phys. Lett.*, vol. 91, p. 201501, 2007.
- [3] Y. Zhao, S. Lin, A. A. Nawaz, B. Kiraly, Q. Hao, Y. Liu, and T. J. Huang, "Beam bending via plasmonic lenses," *Opt. Exp.*, vol. 18, no. 22, pp. 23458–23465, 2010.
- [4] X. Hu and C. T. Chan, "Photonic crystals with silver nanowires as a near-infrared superlens," *Appl. Phys. Lett.*, vol. 85, p. 1520, 2004.
- [5] N. Engheta, A. Salandrino, and A. Alu, "Circuit elements at optical frequencies: Nanoinductors, nanocapacitors, and nanoresistors," *Phys. Rev. Lett.*, vol. 95, p. 095504, Aug. 2005.
- [6] R. Merlin, "Radiationless electromagnetic interference: Diffractive evanescent-field lenses and perfect focusing," *Sci.*, vol. 317, pp. 927–929, Aug. 2007.
- [7] A. Grbic and R. Merlin, "Near-field focusing plates and their design," *IEEE Trans. Antennas Propag.*, vol. 56, pp. 3159–3165, Oct. 2007.
- [8] E. D. Palik, *Handbook of Optical Constants of Solids*. New York, NY, USA: Academic, 1995.
- [9] Y. Tsuji and M. Koshiba, "Finite element method using port truncation by perfectly matched layer boundary conditions for optical waveguide discontinuity problems," *J. Lightw. Technol.*, vol. 20, no. 3, pp. 463–470, Mar. 2002.
- [10] C. E. Rubio-Mercedes and H. E. Hernández-Figueroa, "Padé boundary conditions for the finite-element solution of arbitrary planar junctions," *J. Lightw. Technol.*, vol. 22, pp. 669–676, 2004.
- [11] C. E. Rubio-Mercedes, V. F. Rodríguez-Esquerre, A. M. Ferreira Frasson, and H. E. Hernández-Figueroa, "Novel FEM approach for the analysis of cylindrically symmetric photonic devices," *J. Lightw. Technol.*, vol. 27, pp. 4717–4721, 2009.
- [12] V. F. Rodríguez-Esquerre, D. F. Rego, E. Telmo, C. E. Rubio-Mercedes, C. Aparecida, and H. E. Hernández-Figueroa, "Analysis and desing of subwavelength focusing by cylindrical lenses," in *Proc. Ann. IMOC 2009 – Int. Microwave and Optoelectronic Conf. IEEE*, Belém, PA, 2009.

Cosme E. Rubio-Mercedes was born in Otuzco-Peru, on April 01, 1969. He received the B.S. degree in sciences physics and mathematics with mention in mathematics from the National University of Trujillo UNT, Trujillo-Peru, in 1995 and the M.Sc. and Ph.D. degrees in electrical engineering in 1997 and 2002, respectively, from the State University of Campinas-UNICAMP, Sao Paulo, Brazil.

He was a post-doctoral Research Fellow at the School of Electrical and Computer Engineering, Department of Microwaves and Optics, UNICAMP, Campinas-SP, Brazil from 2003 until January 2004. Currently, he is an adjunct Professor at the Center of Exact Sciences and Technology, State University of Mato Grosso do Sul (UEMS), Dourados-MS, Brazil. He was a post-doctoral research fellow at the North Dakota State University in 2011. His current research interest includes partial differential equations, numerical analysis and numerical methods for engineering. The numerical methods of interest are the finite element and the finite difference methods for electromagnetic fields analysis in conventional and in nanophotonics and nanoplasmatics structures.

Vitaly F. Rodríguez-Esquerre (M'05) was born in Peru, on February 4, 1973. He received the B.S. degree in electronic engineering from the University Antenor Orrego UPAO, Trujillo, Peru, in 1994, revalidated as Electrical Engineer by the Federal University of Minas Gerais UFMG in 2009, and the M.Sc. and Ph.D. degrees in electrical engineering in 1998 and 2003, respectively, from the University of Campinas, Sao Paulo, Brazil.

He was a post-doctoral research fellow at the Division of Media and Network Technologies, Hokkaido University, Japan from 2003 until 2005 and he also was a post-doctoral research fellow at the Department of Microwaves and Optics, Unicamp, Brasil from 2005 until February 2006. He was an Adjunct Professor at the Department of Electrical-Electronic Technology (DTEE) at the Federal Center of Technological Education in Bahia, CEFET-BA, Salvador, Brazil from February 2006 until December 2009. Currently he is an adjunct professor at the Department of Electrical Engineering (DEE) at the Federal University of Bahia, UFBA, Brazil, where was is the Vice-Head of the Electrical Engineering

Department and he is the Vice-Coordinator of the Graduate School of Electrical Engineering. His current research interest includes numerical methods such as the finite element and the finite difference methods for modal and propagation analysis of electromagnetic fields in conventional and photonic crystal integrated optics waveguides, metallo-dielectric nanostructures, metamaterials and subwavelength grating waveguides and devices, integrated optics and optical fibers. He is author and co-author of 12 papers in international journals, 1 book chapter and more than 50 papers in international conferences.

Ivan T. Lima Jr. (S'95–M'04) received the B.Sc. degree in electrical engineering from the Federal University of Bahia (UFBA), Salvador, Brazil, in 1995, the M.Sc. degree in electrical engineering from the State University of Campinas (UNICAMP), Campinas, Brazil, in 1998, and the Ph.D. degree in electrical engineering in the field of photonics from the University of Maryland, Baltimore County, in 2003.

From 1986 to 1996, he was with Banco do Brasil (Bank of Brazil), where he served as the Information Technology Adviser of the State Superintendence of Bahia, Brazil. From 1998 to 2003, he was a Research Assistant with the Optical Fiber Photonics Laboratory, University of Maryland, Baltimore County. He is currently an Assistant Professor with the Department of Electrical and Computer Engineering, North Dakota State University (NDSU), Fargo. He was a post-doctoral research fellow at the University of Campinas in 2011. His research interests have been devoted to the modeling of polarization effects and receivers in optical fiber communications systems and the development of lasers for applications in biotechnology. He has authored or coauthored 33 archival journal papers, 60 conference contributions, one book chapter, and one U.S. Patent.

Dr. Lima received IEEE LEOS Graduate Student Fellowship Award, and he was co-recipient of the Venice Summer School on Polarization Mode Dispersion Award. In February 2004, he was co-instructor of the Short Course (SC210: Hands-on polarization measurement workshop), which was offered at the Optical Fiber Communications Conference and Exposition (OFC) 2004, Los Angeles, CA, USA. In March 2005, he also served as co-instructor of the short courses (SC210-A and SC210-B) at OFC/NOEC 2005, Anaheim, CA. These short courses were sponsored by the IEEE Lasers and Electro-Optics Society (LEOS) and by the Optical Society of America (OSA). He is a member of the IEEE-LEOS and of the OSA.

Hugo E. Hernández-Figueroa (M'94–SM'96 IEEE) received the B.Sc. degree in electrical engineering from the Federal University of Rio Grande do Sul, Porto Alegre, Brazil, in 1983, the M.Sc. degree in electrical engineering and the M.Sc. in informatics, from the Pontifical Catholic University of Rio de Janeiro, Rio de Janeiro, Brazil, in 1985 and 1987, respectively, and the Ph.D. degree in physics from the Imperial College of Science, Technology and Medicine, University of London, U.K., in 1992.

After spending two years as a Postdoctoral Fellow with the Department of Electronic and Electrical Engineering, University College London (UCL), London, U.K., he joined the University of Campinas (UNICAMP), School of Electrical and Computer Engineering (FEEC), Department of Microwaves and Optics (DMO), as an Assistant Professor in 1995. He became Full Professor in 2005 and has been DMO's Head since 2004. He has published about 100 papers in renowned journals and almost 200 international conference papers. He is Co-Editor of the book *Localized Waves: Theory and Applications* (Wiley, 2008). His research interests concentrate on a wide variety of wave electromagnetic phenomena and applications mainly in integrated photonics, nanophotonics, optical fibers, metamaterials, and plasmonics. He is also involved on research projects dealing with information technology applied to technology-based education.

Prof. Hernández-Figueroa has been very active with IEEE (Photonics Society, Microwave Theory and Techniques Society, Antennas and Propagation Society, and Education Society), and also with the Optical Society of America (OSA), acting as organizer for several international conferences, guest editor for special issues, and AdCom member. He founded in 2010 and chairs the first IEEE Photonics Society Brazilian Chapter. He is an Associate Editor (Nanophotonics) of the IEEE Photonics Journal (March 2011–February 2014), and was an Associate Editor (Opto-Electronics/Integrated Optics) of the IEEE/OSA Journal of Lightwave Technology (January 2004–December 2009). He was the General Co-Chair of the OSA Integrated Photonics and Nanophotonics Research and Applications (IPNRA) 2008 topical meeting. He is a Fellow of the OSA 2011 and was a recipient of the IEEE Third Millennium Medal in 2000.